Influence of nitrogen microwave radicals on sequential plasma activated bonding

M.M.R. Howlader [a,*], J.G. Wang [b], M.J. Kim [b]

[a] Electrical and Computer Engineering Department, McMaster University, Hamilton, Ontario, Canada L8S 4K1
[b] Department of Materials Science and Engineering, University of Texas at Dallas, Texas, USA

ARTICLE INFO

ABSTRACT

The role of nitrogen microwave (MW) radicals in sequential plasma activated bonding of silicon/silicon has been investigated through contact angle and electron energy loss spectroscopy (EELS) observations. The contact angle for the sequentially activated (using oxygen RIE time for 60 s followed by variable times of nitrogen MW) silicon surfaces was higher than that of the oxygen RIE activated surfaces below 300 s but it was lower than that of the surfaces treated with oxygen RIE for a prolonged activation of 1200 s. The amorphous layer of the sequentially activated interface became thicker compared to the oxygen RIE treated interface and became thinner after prolonged activation using Nitrogen radicals. The EELS measurements showed no nitrogen in the silicon and interfacial amorphous silicon oxide, but showed oxygen deficiency in the amorphous layer.

© 2009 Elsevier B.V. All rights reserved.

1. Introduction

Low-temperature bonding is crucial for integrating micro-electro-mechanical systems (MEMS) and substrates with temperature-sensitive diverse circuits, components, and devices [1–3]. A sequential plasma activated bonding (SPAB) method that allows for bonding without heating and the application of a high external force has been reported [4–6]. In this method, the wafer surfaces are activated with oxygen (O_2) reactive ion etching (RIE) plasma followed by cleaning with nitrogen (N_2) microwave (MW) radicals in a low vacuum and then bonded in a clean room atmosphere with hand-applied pressure. The high bonding strength achieved without heating is equivalent to or higher than that of hydrophilic and hydrophobic bonding processes done at high temperatures. The combined treatments of N_2 radicals after O_2 RIE showed increased bonding strength over that of O_2 RIE [4–6]. While the absorption of water into bulk silicon without heating increased the bonding strength, the role of nitrogen has not been yet clarified.

The surface hydrophilicity is a measure of the surface energy [7]. The contact angle of a drop of water on the surface allows us to grasp the surface hydrophilicity. The lower the contact angle, the higher the degree of hydrophilicity [8]. Therefore, the comparison of characteristic contact angle behaviors between those of sequentially treated surfaces with N_2 MW radicals and those treated with O_2 RIE plasma are indispensable. Ultimately the surface behaviors control the bonding strength at the interface. To investigate the bonded interface,

electron energy loss spectroscopy (EELS) was used to detect elements present at and to profile the interface [9]. Although hypothetical models were presented in order to explain the role of nitrogen, the EELS of the SPAB interface required to definitively determine nitrogen's role has yet to be done.

This article investigates the role of N_2 radicals in SPAB by measuring the water contact angle on the Si surface and the EELS analysis of the bonded interface.

2. Experimental

P-type double side mirror polished CZ grown (100) Si wafers with thicknesses of 725 μm were used. The resistivity of the wafers was 25–30 Ω-cm. The wafer surfaces were activated in a low vacuum pressure using 13.85 MHz O_2 radio frequency (RF) plasma followed by 2.45 GHz N_2 MW plasma at room temperature. In the case of MW plasma, a metal plate with holes (diameter = 1 mm) was used to extract electrically neutral radicals. Radicals can chemically activate the wafer surfaces. On the other hand, ions generated in RIE in the RF plasma were accelerated by self-bias voltage to increase physical bombardment capability. The RF and MW plasma powers were 200 and 2000 W, respectively.

For sequential activation, the wafer surfaces were processed by O_2 RIE plasma for 60 s at 30 Pa and then subsequently processed by N_2 MW radicals for 60 s at 30 Pa unless otherwise mentioned. Table 1 shows the plasma processing parameters in the O_2 RIE plasma activated bonding process and SPAB process with tensile strength experiments.

After plasma activation, the wafers were taken out of the chamber and bonded in a class 10,000 clean room. The hydrophilicity of the

* Corresponding author. Tel.: +1 905 525 9140x26647; fax: +1 905 523 4407.
E-mail address: mrhowlader@ece.mcmaster.ca (M.M.R. Howlader).

Table 1
Experimental conditions of plasma parameters in the O_2 RIE plasma activated bonding process and in the sequential plasma activated bonding (SPAB) process with bonding strength of the silicon/silicon interfaces.

Activation mode	O_2 RIE Plasma			N_2 MW Radicals			Tensile strength (MPa)
	Power (W)	Time (s)	Pressure (Pa)	Power (W)	Time (s)	Pressure (Pa)	
O_2 RIE	200	10	30	–	–	–	9.06
		60					14.46
		300					16.42
		1200					7.51
SPAB	200	60	30	2000	10	30	15.86
					60		21.04
					300		21.56
					1200		16.56

Fig. 1. (a) Contact angles dependence of a droplet of DI water on Si wafer surface as a function of activation time of N_2 MW radical compared with O_2 RIE plasma and (b) time elapsed behavior of contact angles after plasma activation.

activated surfaces was analyzed by measuring water contact angles. These measurements were accomplished using the sessile drop method with a deionized (DI) water droplet (5 μL) by Kruss Drop Shape Analysis system DSA100. A contact angle below 2° cannot be detected using the specified equipment. Transmission electron microscopy (TEM) cross-section samples were prepared by standard sample preparation techniques with low-energy ion milling as the final step. High resolution TEM (HRTEM), high angle annular dark-field (HAADF)-STEM, and EELS were performed using a field-emission TEM (JEOL 2100F, $C_s = 0.5$ mm) in conjunction with a Gatan Enfina 1000 spectrometer operating at 200 kV. The energy resolution was about 1.0 eV. Typical probe conditions for EELS used in this work consisted of 1.0 nm diameter probe in TEM conditions and a ~0.3 nm diameter probe with a convergence semi-angle of 14mrad in STEM condition. Core-loss EELS spectra of N–K, Si–$L_{2,3}$ and O–K were recorded.

3. Results and discussions

The experimental results of tensile tests (Table 1) showed that the bonding strength of the silicon specimens was increased after sequential activation. For example, the bonding strength of the O_2 RIE plasma treated specimen for 60 s at 30 Pa was 14.46 MPa, which was increased to 21.04 MPa in SPAB using activation with O_2 RIE and N_2 MW radicals both for 60 s at 30 Pa. For prolonged activation both in the O_2 RIE plasma and SPAB, the bonding strength of the specimens after O_2 RIE plasma activation for 1200 s at 30 Pa was 7.51 MPa, while the bonding strength of the specimens activated by N_2 MW radical for 1200 s at 30 Pa after O_2 RIE plasma was 16.56 MPa.

In order to understand the influence of N_2 radicals on improving bonding strength, the water contact angles of silicon surfaces activated using the plasma-processing parameters of N_2 MW radicals (i.e., plasma time) and O_2 RIE were investigated. Fig. 1(a) shows the contact angles on Si wafer surface as a function of activation time of N_2 MW radicals compared with O_2 RIE plasma. For the O_2 RIE plasma, the power and pressure were 200 W and 50 Pa. The parameters of sequential activation were a 200 W O_2 RIE for 60 s at 50 Pa followed by a 2000 W N_2 MW radicals at 50 Pa for variable times. The processing time dependence of surface activation on the contact angle showed that the contact angle of the activated surfaces both in the O_2 RIE and sequential activation was higher than that of the non-activated surface. The contact angle was monotonously changed with processing activation time. A prolonged activation of 1200 s reduced contact angles in both N_2 MW radicals and O_2 RIE, but they were higher than that of non-activated surface. The surface activation below 300 s and at 1200 s showed significant differences in the contact angle. The higher contact angle in the sequential activation before 300 s showed less hydrophilic surfaces compared to that of the O_2 RIE. While this results in decreased surface energy in the sequential
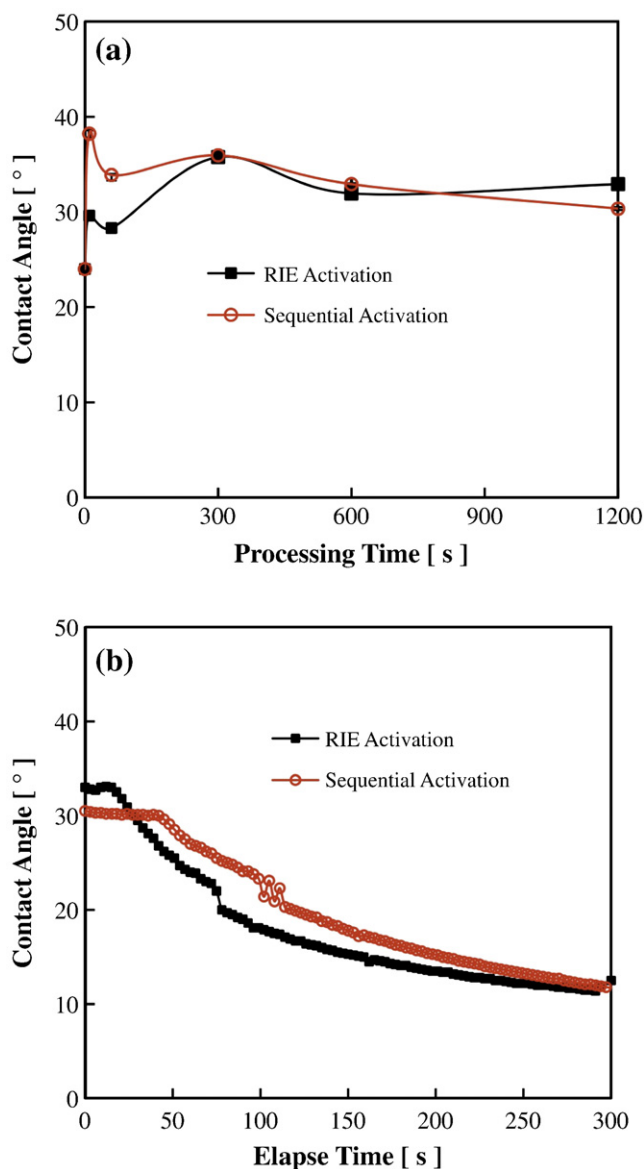
activation, the bonding strength was increased at this condition. The characteristic behavior of the contact angle is attributed to the surface roughness [10]. Fig. 1(b) shows time elapsed behavior of the contact angle of O_2 RIE and sequential activated surfaces both after 1200 s treatment. Note that the sequential activation was done after 60 s of O_2 RIE activation. While the contact angles right after activation in the RIE was higher than that in the sequential, they were decreased after 50 s and identical at 300 s. Time dependent behaviors of contact angles after plasma activation indicate sequentially treated surfaces have greater chemical reactivity over that of RIE treated surfaces. At these conditions, the nanostructure behavior of the interface with elemental distribution allows further insight into the role of N_2 on the increased surface energy and high bonding strength.

Fig. 2 shows the HRTEM images of SPAB interface compared with the RIE bonded interfaces. The thickness of the amorphous intermediate layers of the SPAB bonded interface was thicker than that of the RIE processed interface. The thickness of the amorphous layer for prolonged activation (N_2 radicals for 1200 s) was lower than that of
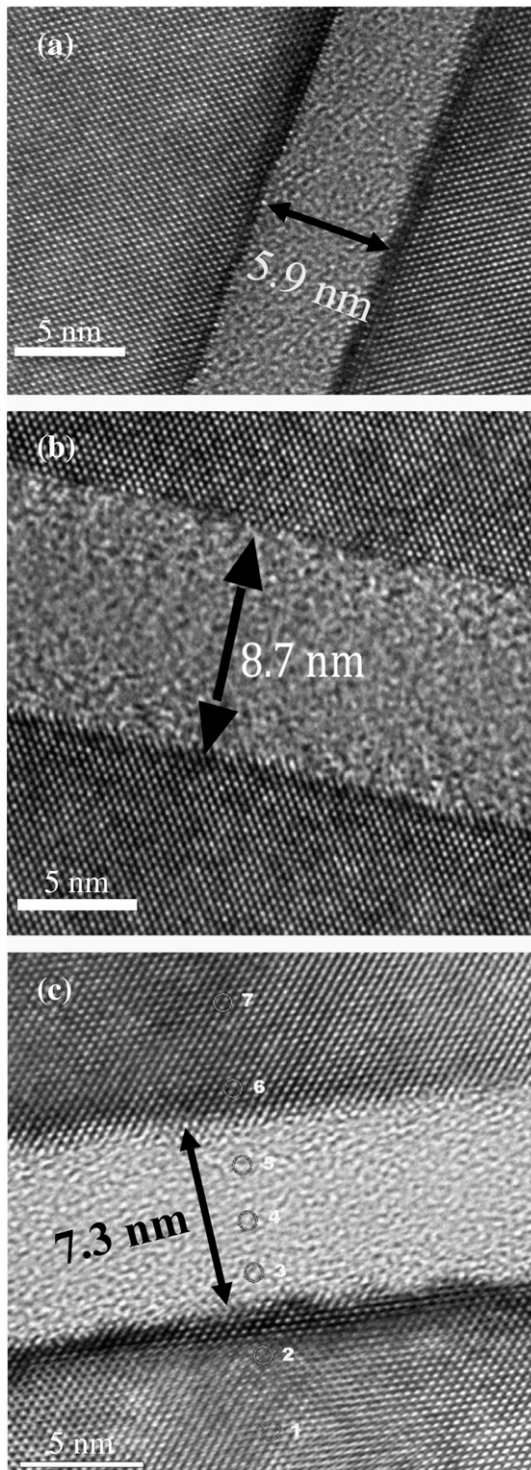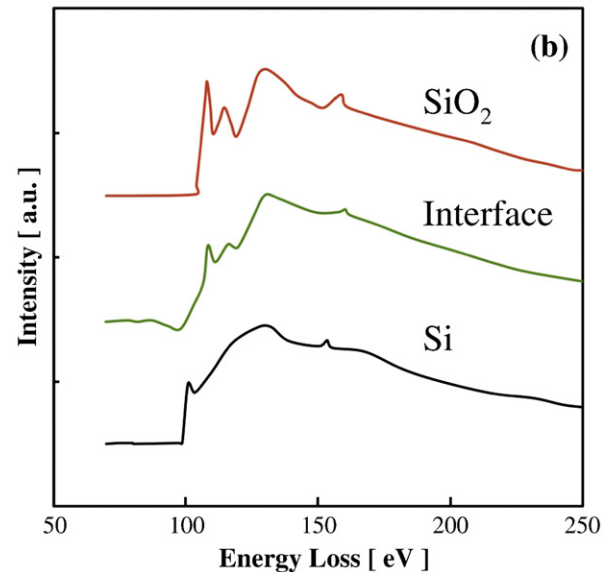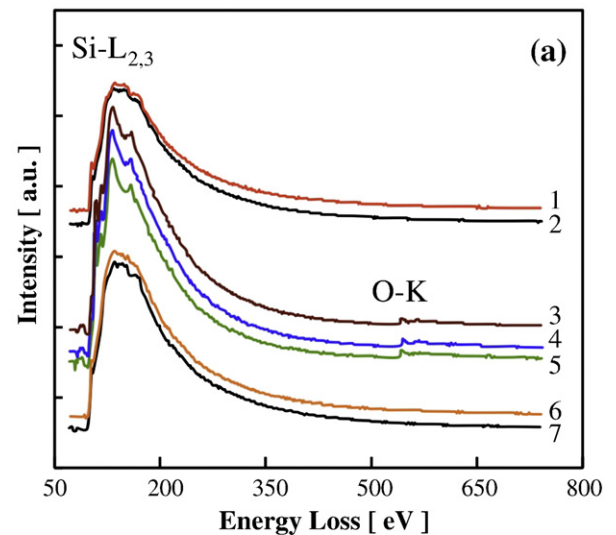
Fig. 2. HRTEM images of Si/Si wafers bonded by (a) the O_2 RIE plasma activation for 60 s at 30 Pa, (b) the O_2 RIE plasma activation for 60 s at 30 Pa followed by N_2 MW radicals for 10 s at 30 Pa, and (c) the O_2 RIE plasma activation for 60 s at 30 Pa followed by N_2 MW radicals for 1200 s at 30 Pa.

predominantly increase porosity in the amorphous layer. The presence of these layers can be attributed to the shrinkage of amorphous layers.

Fig. 3(a) shows the EELS from the spots marked on the image of Fig. 2(c) at locations 1 to 7 for detection of elements at the interface. Prolonged activation reduced the thickness of the amorphous layer to 7.3 nm. The reduced thickness of the amorphous layers can be understood through the elemental detection at the bonded interface using the EELS spectra that were done at locations 1 to 7. The locations at point 1, 2, 6, and 7 indicate pure Si. The locations at points 3, 4, and 5 indicate the bottom, middle, and top positions of the oxide layer, respectively. No nitrogen was detected in all the locations [12,13]. If nitrogen was present, the nitrogen concentration may be below the detection limit of EELS. The Si–$L_{2,3}$ edges at 125–175 eV were observed both in the silicon and amorphous oxide layer. The Si–$L_{2,3}$ edges from all the measured locations at amorphous oxide layer were almost identical. The O–K edges at 540–560 eV were observed only in amorphous oxide layer at the interface. Further analysis of the Si–$L_{2,3}$ of amorphous layer compared with standard Si and SiO_2 provides the

Fig. 3. (a) the EELS from the spots marked on the Fig. 2(c) at locations 1 to 7; (b) the Si–$L_{2,3}$ edges of the Si, SiO_2 and the interfacial amorphous oxide layer at location 4.
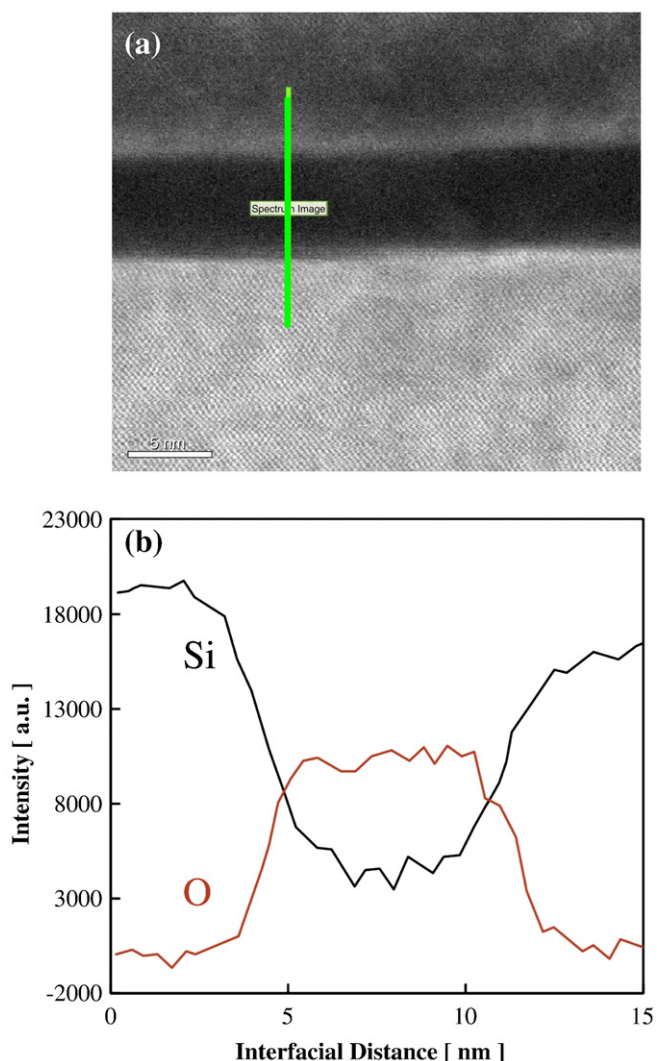
shorter activation (N_2 radicals for 10 s) sample. This prolonged surface activation made the surfaces hydrophilic by covering the reactive surfaces with SiO_xN_y and OH^- molecules [4,10,11]. Since the bonding was accomplished in the ambient outside the plasma chamber, OH^- molecules from the ambient also contributed to the hydrophilicity of the bonded interface. Prolonged activation with N_2 radicals after O_2 RIE plasma may lead to chemical reactions, which

Fig. 4. (a) HAADF images of Si/Si wafers bonded interface; (b) STEM–EELS spectrum imaging line profile across the interface amorphous layer. Vertical line indicates the EELS scan position.

characteristic behavior of amorphous layer at the interface. Fig. 3(b) shows the Si–$L_{2,3}$ edges from the interfacial amorphous oxide layer at location 4 compared with that of the standard Si and SiO_2. It is well known that the electron energy loss near-edge fine structure (ELNES) of Si–$L_{2,3}$ edge is the fingerprint of the bonding and electronic structure of Si elements [14]. Comparing the Si–$L_{2,3}$ edges from the standard Si and SiO_2, the Si–$L_{2,3}$ edges from the amorphous SiO_2 features a Si with a valence between Si^0 and Si^{4+}, which implies that silicon suboxides (SiO_x, $x<2$) were present at the interface.

Fig. 4(a) shows a HAADF image of the Si/Si bonded interface. Identical thickness of the amorphous layer at the interface to that of using HRTEM was observed (shown in Fig. 2(c)). Fig. 4(b) shows a STEM–EELS spectrum imaging line profile across the interface amorphous layer, in which Si–$L_{2,3}$ and O–K edges were recorded to form the line profiles. Spectra have been recorded at 0.5 nm intervals along the 13 nm line trace shown in Fig. 4(a). All spectra have been calibrated to the zero loss peak (ZLP) and deconvoluted to remove multiple scattering influences. The spectrum for silicon reduces with approaching to the interface and becomes constant with lowest amplitudes through the interface. The spectrum for oxide increased with approaching to the interface and becomes constant with highest amplitudes through the interface. The scanning for elemental distribution of Si and O across the whole interface also showed no proportional distribution, which supports to the Si suboxides amorphous layer at the whole interface amorphous layer.

4. Conclusions

The water contact angle measurements showed that the sequentially treated surfaces with O_2 RIE and nitrogen MW radicals had lower contact angle than that of O_2 RIE processed specimens when the activation time was 1200 s. This reduced contact angle provides higher hydrophilicity in the sequential activation than that in the O_2 RIE. The amorphous layer of the sequentially activated interface became thicker compared to the O_2 RIE treated interface and it was thinner after prolonged activation using N_2 radicals. The EELS measurements for prolonged activation times with MW N_2 radicals showed that no nitrogen was detected both in the silicon and interfacial silicon oxide. The amorphous Si oxide seems more like oxygen deficient.

References

[1] Christiansen SH, Singh R, Gösele. Proc IEEE 2006;94:2060–105.
[2] Suni T, Henttinen K, Lipsanen A, Dekker J, Luoto H, Kulawski M. J Electrochem Soc 2006;153:G78–82.
[3] Farrens SN, Dekker JR, Smith JK, Roberds BE. J Electrochem Soc 1995;142:3949–55.
[4] Suga T, Kim TH, Howlader MMR. Proc 54th Electron Compon Technol conf; 2004. p. 484–90.
[5] Howlader MMR, Suehara S, Suga T. Sens Actuators A 2006;127:31–6.
[6] Howlader MMR, Suehara S, Takagi H, Kim TH, Maeda R, Suga T. IEEE Trans Adv Packaging 2006;29:448–56.
[7] Bhattacharya S, Datta A, Berg JM, Gangopadhyay S. J Microelectromech Syst 2005;14:590–7.
[8] Ma X, Chen C, Liu W, Liu X, Du X, Song Z, et al. J Electrochem Soc 2009;156:H307–10.
[9] Grundner M, Jacob H. Appl Phys A 1986;A39:73–82.
[10] Howlader MMR, Suga T, Itoh H, Kim MJ. ECS Trans 2006;3:191–202.
[11] Howlader MMR, Suga T, Itoh H, Lee Th, Kim MJ. J Electrochem Soc 2009;156: H846–51.
[12] Sekiguchi T, Kimoto K, Aoyama T, Mitsui Y. Jpn J Appl Phys 1998;37:L694–6.
[13] Gritsenko VA, Svitasheva SN, Petrenko IP, Wong H, Xu JB, Wilson IH. J Electrochem Soc 1999;146:780–5.
[14] Batson PE. Nature 1993;366:727–8.